**Supplemental Data**

**Supplementary Table 1: Pairwise comparisons of *Nfi*$^{-/-}$ hippocampal microarrays using hypergeometric tests**

List of unique genes and shared genes (>1.5 fold change) upon comparing *Nfix*$^{-/-}$ and *Nfib*$^{-/-}$ microarrays, *Nfix*$^{-/-}$ and *Nfia*$^{-/-}$ microarrays, *Nfib*$^{-/-}$ and *Nfia*$^{-/-}$ microarrays. The *P* value for each comparison was determined using a hypergeometric test.

| Microarray pairwise comparison | Number of unique misregulated genes (>1.5 Fold change) | Number of shared misregulated genes (>1.5 Fold Change) | *P* value |
|---|---|---|---|
| *Nfix*$^{-/-}$ and *Nfib*$^{-/-}$ E16.5 hippocampus | *Nfix* (430), *Nfib* (1645) | 248 | $P < 1*10^{-320}$ |
| *Nfix*$^{-/-}$ and *Nfia*$^{-/-}$ E16.5 hippocampus | *Nfix* (466), *Nfia* (887) | 212 | $P < 1*10^{-320}$ |
| *Nfib*$^{-/-}$ and *Nfia*$^{-/-}$ E16.5 hippocampus | *Nfib* (1162), *Nfia* (431) | 731 | $P < 1*10^{-320}$ |

**Supplemental Table 2: Common misregulated genes in *Nfi*$^{-/-}$ hippocampal microarrays, related to Figure 6.**

List of genes misregulated >2.5 fold change ($p$ <0.05) in all three E16.5 hippocampal datasets: *Nfix*$^{-/-}$ (Heng et al., 2014), *Nfib*$^{-/-}$ (Piper et al., 2014) and *Nfia*$^{-/-}$ (Piper et al., 2010).

| Gene name | Fold change E16.5 *Nfix*$^{-/-}$ Hipp | Fold change E16.5 *Nfib*$^{-/-}$ Hipp | Fold change E16.5 *Nfia*$^{-/-}$ Hipp |
|---|---|---|---|
| *Adra2a* | -4.054 | -3.464 | -3.770 |
| *Ca3* | -3.028 | -6.553 | -4.450 |
| *Caln1* | -3.833 | -2.530 | -2.518 |
| *Cpne9* | -8.373 | -8.293 | -7.267 |
| *Entpd2* | -4.641 | -6.316 | -5.740 |
| *Fn1* | 2.618 | 3.401 | 2.833 |
| *Gal* | -4.976 | -4.996 | -5.430 |
| *Gfap* | -6.838 | -7.294 | -17.330 |
| *Grp* | -9.031 | -8.705 | -11.420 |
| *Hey2* | 2.647 | 2.933 | 2.571 |
| *Il16* | -2.919 | -2.986 | -3.087 |
| *Il31ra* | 2.769 | 2.646 | 2.710 |
| *Insc* | -2.739 | -5.659 | -6.452 |
| *Kcnk1* | -4.154 | -3.053 | -3.723 |
| *Ncam1* | -2.799 | -3.817 | -5.102 |
| *Rasd2* | -2.940 | -6.018 | -4.421 |
| *Sphk1* | -2.875 | -2.552 | -2.700 |

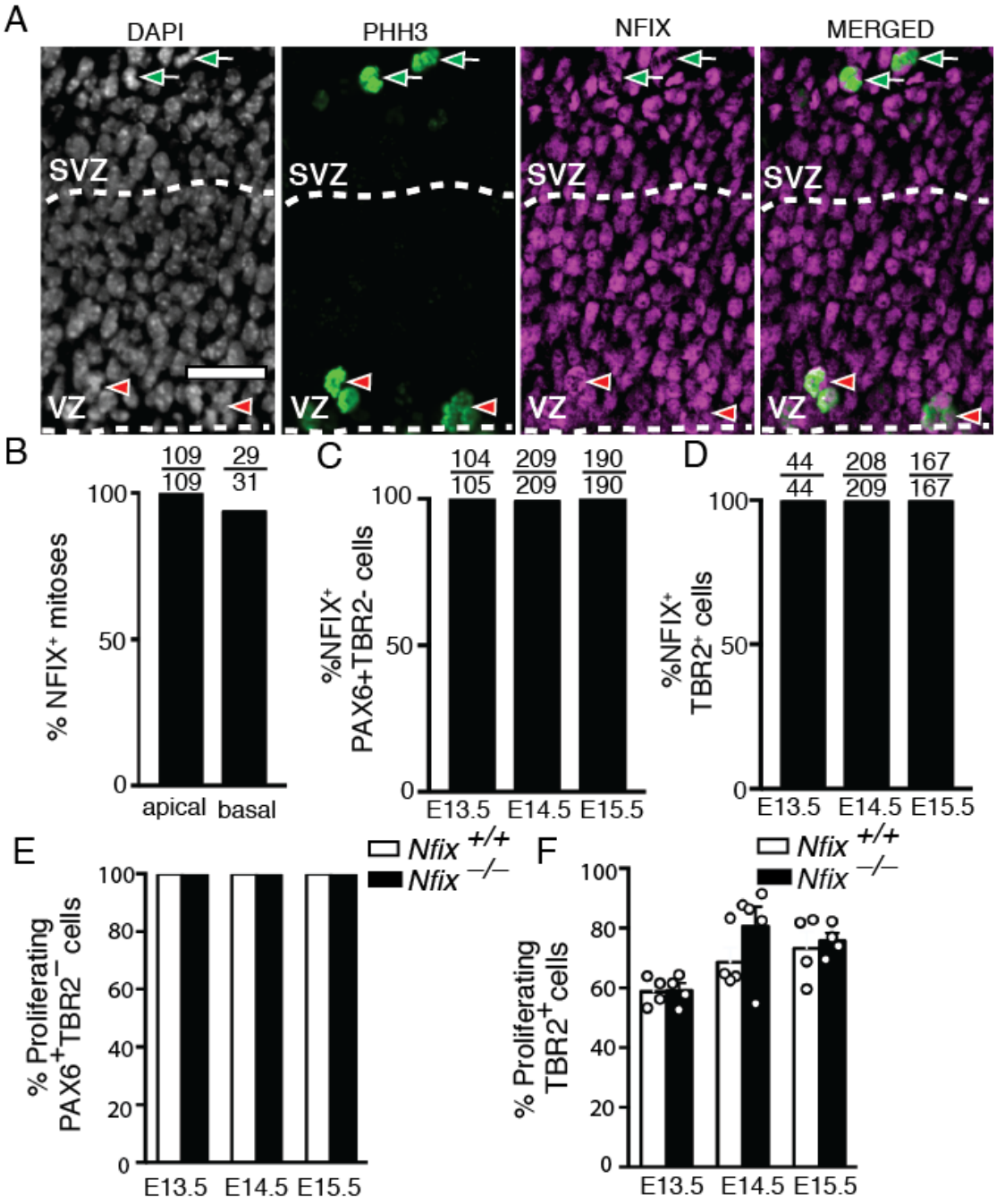


**Supplementary Figure 1: NFIX is expressed during mitosis, related to Figure 1.**
(A) NFIX immunofluorescence at the level of the hippocampus at E14.5. Dashed lines demarcate the ventricular zone (VZ)/subventricular zone (SVZ). NFIX (magenta) colocalizes with the mitotic marker PHH3 (green). Red arrowheads indicate radial glia undergoing mitosis and green arrows indicate IPCs undergoing mitosis. Scale bar (in A)**:** A, 50 µm. Quantification of the percentage of $NFIX^+$ (B) apical and basal mitoses, (C) radial glia and (D) IPCs at E14.5. (E) The percentage of radial glia and (F) the percentage of IPCs that are proliferating in wild-type and *Nfix*$^{-/-}$ mice from E13.5-E15.5. Graphs depict mean ± SEM of at least 4 embryos.

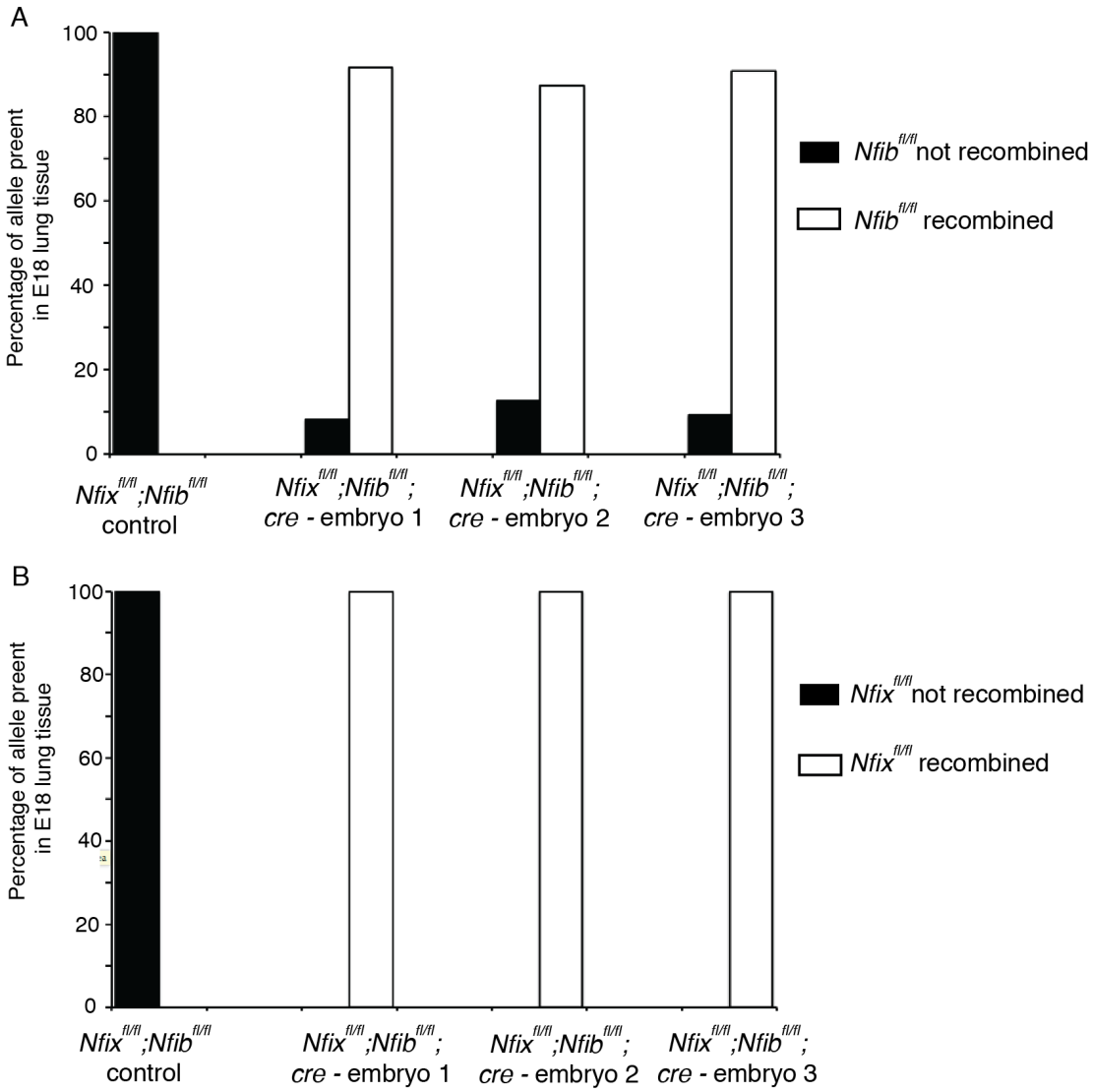


**Supplementary Figure 2. Incomplete recombination of *Nfib*$^{fl/fl}$ allele in *Nfix*$^{fl/fl}$; *Nfib*$^{fl/fl}$; *Rosa26creER*$^{T2}$ mice upon tamoxifen administration, related to Figure 5.**
(A) qPCR DNA analysis of *Nfib*$^{fl/fl}$ recombination efficiency in *Nfix*$^{fl/fl}$; *Nfib*$^{fl/fl}$; cre mice and *Nfix*$^{fl/fl}$; *Nfib*$^{fl/fl}$ controls from lung tissue. Black bars depict percent of allele that is not recombined, and white bars depict percentage of allele that is recombined. (B) qPCR DNA analysis of *Nfix*$^{fl/fl}$ recombination efficiency as performed in (A).

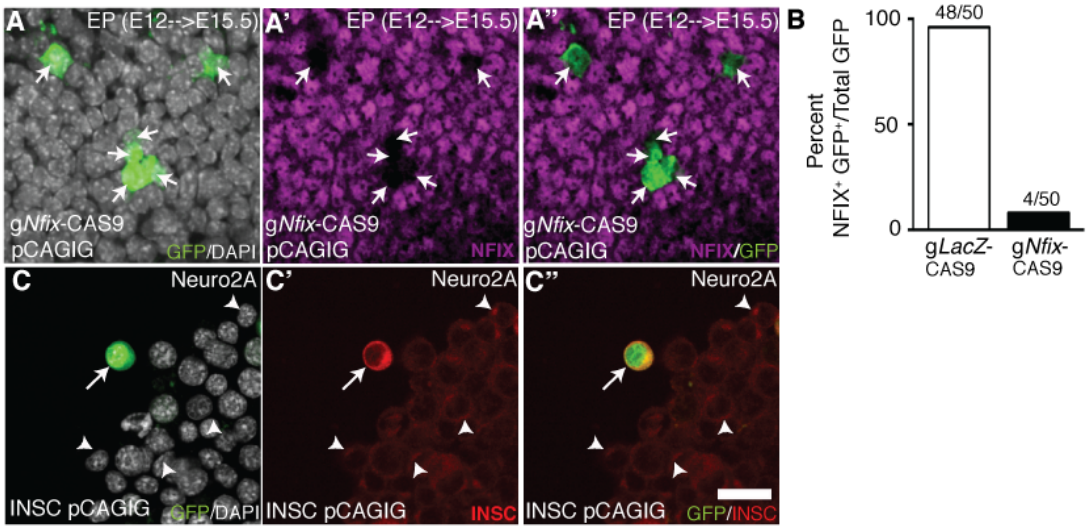


**Supplementary Figure 3. Validation of g*Nfix*-CAS9 and INSC pCAGIG constructs**

(A-A") DAPI (white), GFP (green) and NFIX (magenta) in E15.5 CD1 wild-type mice electroporated at E12.5 with *gNfix*-CAS9 and pCAGIG constructs. Arrows indicate electroporated cells that are negative for NFIX. (B) Cell counts of the proportion of electroporated cells expressing NFIX in the control condition (g*lacZ*-CAS9 and pCAGIG) and knockout condition (*gNfix*-CAS9 and pCAGIG). (C) DAPI (white), GFP (green) and INSC (red) in Neuro2A cells transfected with INSC pCAGIG and analysed 48h later. Arrow indicates transfected cell expressing high levels of INSC, arrowheads indicate low endogenous levels of INSC in non-transfected cells (arrowheads). Scale bar (in C"): A 18.5µm, B 22µm.

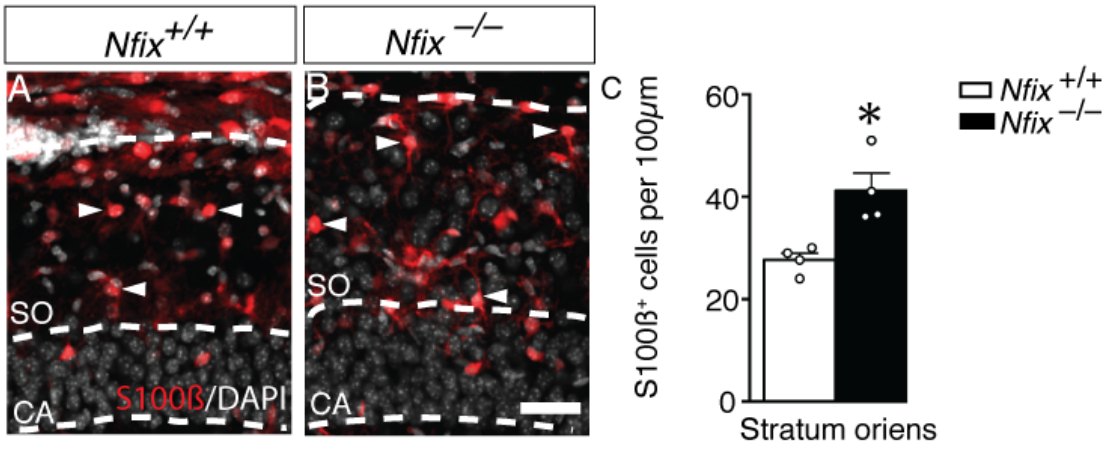


**Supplementary Figure 4. Increased astrocyte number in the stratum oriens of P15 *Nfix*$^{-/-}$ mice, related to Figure 8.**

(A) and (B) show DAPI (white) and S100ß (red) in wild-type and *Nfix*$^{-/-}$ hippocampi at P15, with the dashed lines demarcating the boundary of ammons horn (CA) neuronal layer and the stratum oriens (SO) neuropil. (C) Cell counts of the number of S100ß$^{+}$ astrocytes in the SO layer. Graphs depict mean ± SEM from 4 embryos *$p$ < 0.05 ($t$ test). Scale bar (in B): A, B 40 µm.

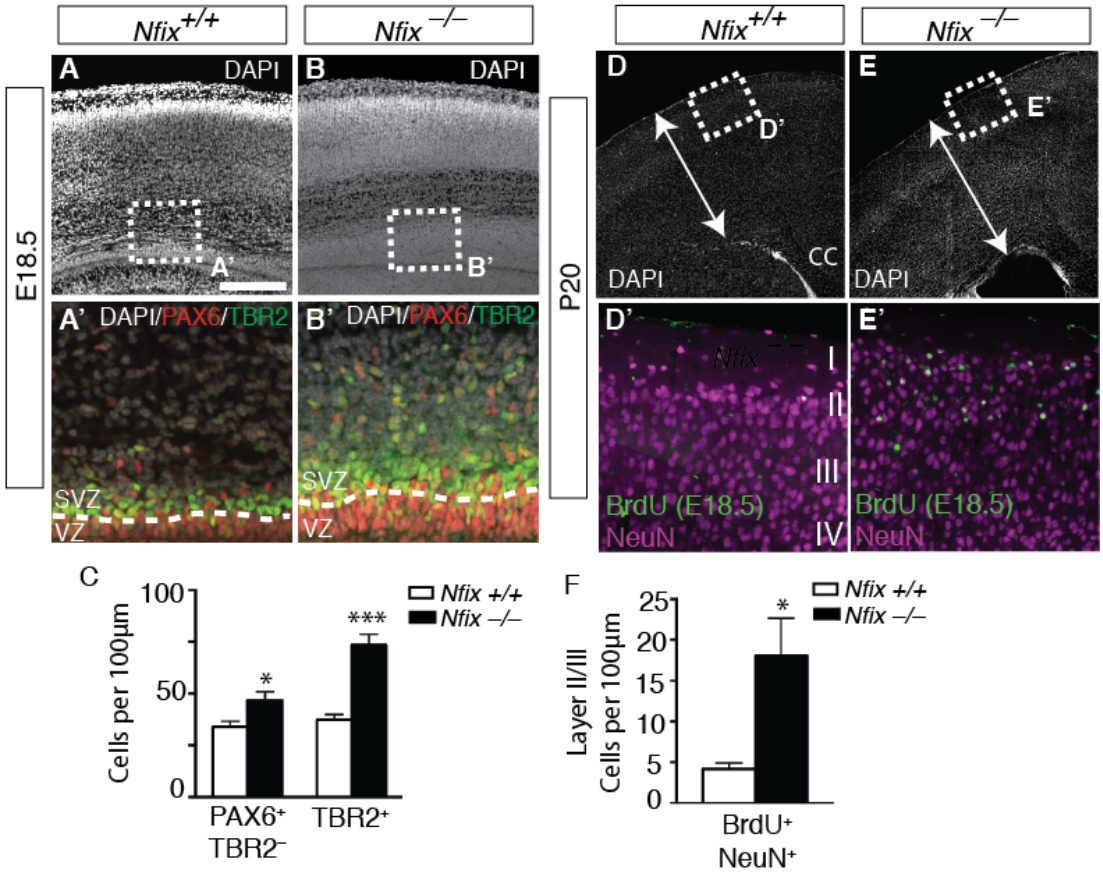


**Supplementary Figure 5. Prolonged neurogenic window increases neuron number in the neocortex of *Nfix*$^{-/-}$ mice, related to Figure 8**

(A) and (B) show DAPI (white) staining in wild-type and *Nfix*$^{-/-}$ neocortices at E18.5. The boxed regions in (A) and (B) are shown at a higher magnification in (A') and (B') respectively, showing DAPI (white), PAX6 (red) and TBR2 (green) expression, with the dashed lines demarcating the ventricular zone (VZ)/subventricular zone (SVZ) boundary. (C) Radial glia and IPC counts in the E18.5 cortex of wild-type and *Nfix*$^{-/-}$ mice. Graphs depict mean ± SEM of 5 embryos * $p < 0.05$, *** $p < 0.001$ (*t* tests). (D) and (E) show DAPI (white) staining in wild-type and *Nfix*$^{-/-}$ neocortices at P20, with arrows spanning the neocortex from pial surface to the ventricular surface. The boxed regions in (D) and (E) are shown at a higher magnification in (D') and (E') respectively, showing BrdU-positive cells (green), which were birthdated at E18, and NeuN staining (magenta), in the upper layers of the cortical plate. (F) Quantification of the number of BrdU$^{+}$NeuN$^{+}$ layer II/III cells in wild-type and *Nfix*$^{-/-}$ mice. Graphs depict mean ± SEM of 5 embryos * $p < 0.05$ (*t* test). Scale bar (in A) A, B 200 µm; A', B' 50 µm; C, D 375 µm; C', D' 62.5 µm.

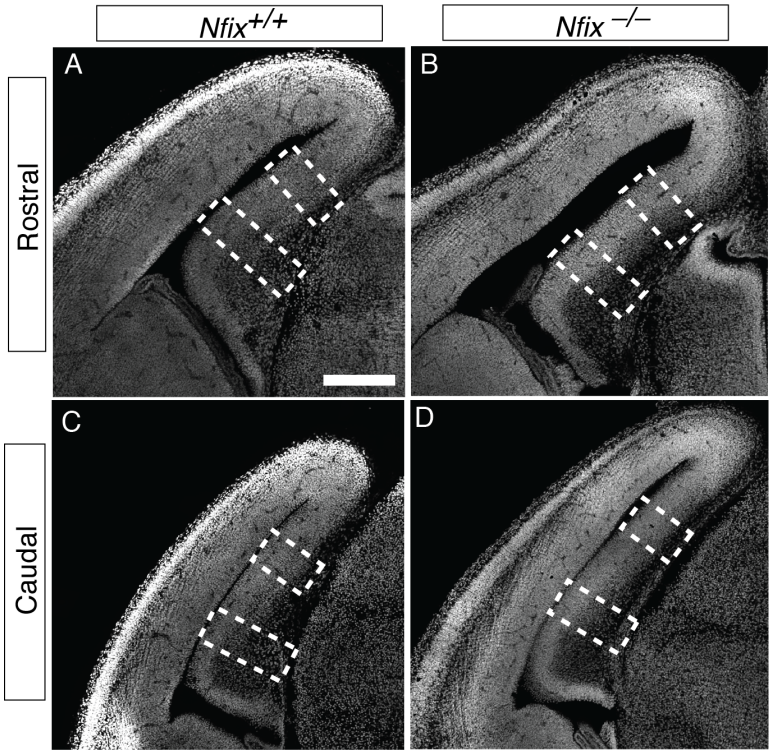


**Supplementary Figure 6: Sampling areas for hippocampal cell counts, related to Figures 2-4.**

(A-D**)** Representative rostral and caudal E14.5 coronal sections of *Nfix*$^{+/+}$ (A, C) and *Nfix*$^{-/-}$ (B, D) mouse brains stained with DAPI (white). To perform the cell counts described in this manuscript, we analysed a rostral and a caudal section for each animal at each age investigated. For each section the number of immunopositive cells in two equally spaced 100 µm sampling columns spanning the dorsal-ventral width of the ammonic neuroepithelium (boxed areas in A-D) were quantified.

Scale bar (in A)**:** A,B 250 µm, C, D 300 µm.

## Supplementary Materials and Methods

### Immunofluorescence and immunohistochemistry

Embryos were immersion-fixed at E14.5 or younger in 4% paraformaldehyde (PFA) or perfused transcardially (E15.5 and older) with phosphate-buffered saline (PBS), followed by 4% PFA, then post-fixed for 48-72 h before long term storage in PBS at 4°C. Brains were embedded in noble agar and sectioned in a coronal plane at 50 µm using a vibratome (Leica, Deerfield, IL). Sections were mounted on slides before heat-mediated antigen retrieval was performed in 10 mM sodium-citrate solution at 60°C for 20 min (for GFP and TBR2 immunostaining) or 95°C for 15 min (for all other co-immunostaining). A standard fluorescence immunohistochemistry protocol was then performed. Briefly, sections were covered in a blocking solution for 2 h containing 2% normal serum and 0.2% Triton-X-100 made in PBS. The primary antibodies were diluted in this blocking solution and incubated with the sections overnight at 4°C. The following day the primary antibodies were detected with fluorescently conjugated secondary antibodies diluted in block for 2 h. When dual or triple labelling was being performed the secondary antibodies used were derived from the same species to prevent cross-species reactivity. Sections were then counterstained with DAPI (Invitrogen, Carlsbad, CA) and coverslipped using DAKO fluorescent mounting media. Chromogenic immunohistochemistry using 3,3'-diaminobenzidine was performed as above but with a goat anti-rabbit biotin-conjugated secondary antibody. The reaction was visualised by incubating the sections in avidin-biotin complex (ABC elite kit; Vector Laboratories, Burlingame, CA) for 1 h, followed by a nickel-DAB solution, and was terminated by washing multiple times in phosphate buffered saline when a purple precipitate had formed.

### Primary antibodies

The primary rabbit species antibodies used were anti-PAX6 (AB2237 1/400, Millipore, Billerica, MA), anti-NFIX (AB101341 1/500, Abcam Cambridge, UK), anti-NFIB (HPA003956 1/200 Sigma-Aldrich, St Louis, MO) anti-PHH3 (#06-570 1/200, Millipore), anti-NeuN (EPR12763 1/800, Abcam), anti-TBR2 (ab23345, 1/800, Abcam), anti-S100ß 647 (ab1961175, 1/400, Abcam) and anti-INSC (gift from Juergen Knoblich) (Zigman et al., 2005). The primary mouse species antibodies used were anti-BrdU (G3G4 1/100, DHSB, Iowa city, IA), anti-NFIX clone 3D2

(SAB1401263 1/400, Sigma-Aldrich), anti-NeuN (MAB377 1/150, Millipore) and anti-alpha-tubulin (ab7291 1/400 Sigma-Aldrich). The primary rat species antibodies used were anti-Ki67 FITC clone SolA15 (11-5698-80 1/400, San Diego, CA), anti-EOMES (TBR2) Alexa Fluor® 488 (53-4875-82 1/400, Ebioscience). The primary chicken species antibody used was anti-GFP (A10262, 1/500, Thermo Fisher Scientific).

### *Nfix*$^{-/-}$ mouse hippocampal cell counts

For counts of PAX6$^{+}$ TBR2$^{-}$ nuclei and TBR2$^{+}$ nuclei the number of immunopositive cells from two 100 µm sampling fields, spanning the width of the hippocampal primordium, positioned along the medial to lateral extent of the hippocampal ammonic neuroepithelium (E13.5-E18.5) or neocortex (E18.5) were counted. This analysis was completed at two different levels along the rostrocaudal axis for each brain examined. Fluorescent images were captured using a 20X objective on a Zeiss inverted Axio-Observer fitted with a W1 Yokogawa spinning disk module and Hamamatsu Flash4.0 sCMOS camera using 3i Slidebook software (Denver, CO).

### *Nfix*$^{-/-}$ mouse birth-dating experiments

Two birth-dating experiments were performed with 5-bromo-2'deoxyuridine (BrdU, Sigma-Aldrich) in this study. In the first experiment, pregnant dams were injected with low-dose (50 mg/kg) or high-dose (200 mg/kg) BrdU at E13.5 and embryos were perfused 24 h or 48 h later, respectively. The 200 mg/kg dose, while high, has been used in previous studies (Kempermann et al., 1997; Cameron and McKay, 2001; Seib et al., 2013) and has been demonstrated to be within the upper range of acceptable doses for such experiments (Wojtowicz and Kee, 2006). This dose of BrdU ensured the continued labelling of radial glia despite multiple rounds of cellular division during this period. The number of BrdU$^{+}$ cells that labeled as PAX6$^{+}$ TBR2$^{-}$ or Ki67$^{-}$ at E15.5 was calculated as a proportion of the total number of BrdU$^{+}$ cells. Cell counts were performed from two 100 µm sampling fields spanning the width of the hippocampal primordium at two different levels along the rostrocaudal axis of the ammonic neuroepithelium. Fluorescent sections for this experiment were imaged using a 40X objective on a spinning disk confocal microscope. In the second birth-dating experiment, pregnant dams were injected with a standard dose (50 mg/kg) of BrdU at E18.5 and the resulting litter was collected at P20. This dose of BrdU was

sufficient to label neurons generated at E18.5. The total number of $BrdU^+NeuN^+$ cells in CA neuronal layers, and layer II/III of the neocortex was then calculated from a 100 µm sampling field. For the CA counts this was performed on three different levels along the rostrocaudal axis of the brain, in both the CA1 and CA3 neuronal layer and averaged. The neocortical counts were performed on single section at the level of the corpus callosum. Fluorescent sections for this experiment were imaged using a 20X objective on a spinning disk confocal microscope. For both birth-dating experiments the pattern of BrdU staining depended on the chromatin structure at time of fixation, and was pan-nuclear during S-phase or in post-mitotic cells, and punctate during G2/M phase, thus $BrdU^+$ cells were scored as any nuclei showing nuclear immunoreactivity regardless of the staining pattern.

**Measurement of cell cycle kinetics in *Nfix*$^{-/-}$ radial glia**

The mean total cell cycle ($T_C$) and synthesis (S) phase duration ($T_S$) of radial glia in the ammonic neuroepithelium at E14.5 was determined using a dual-pulse labeling protocol modified from the methodology presented by Martynoga and colleagues (2005). Briefly, pregnant dams were injected with 50 mg/kg of 5-ethynyl-2'-deoxyuridine (EdU), followed 1 h later with 50 mg/kg BrdU. At 1.5 h post-EdU injection the dam was sacrificed and embryos immersion-fixed in 4% PFA. Sections were stained for BrdU, EdU, TBR2 and DAPI. Fluorescent sections were imaged using a 40X objective on a spinning disk confocal microscope, and cell counts were performed from two 100 µm sampling fields at each of two different levels along the rostrocaudal axis per brain (Supp Fig. 6). Radial glia were then identified as $TBR2^-$ nuclei located in the ventricular zone. The pattern of BrdU and EdU staining depends on the chromatin structure at time of fixation, and is pan-nuclear during S-phase, and punctate during G2/M phase. $BrdU^+$ and $EdU^+$ radial glia were therefore scored as any nuclei showing immunoreactivity for these markers regardless of the staining pattern. The $T_S$ of radial glia is equal to the injection interval of 1 h multiplied by the ratio of radial glia that remain in S-phase to the number of radial glia that leave S-phase prior to BrdU injection, given by the equation $T_S = 1*(EdU^+BrdU^+/EdU^+BrdU^-)$. The $T_C$ of radial glia is equal to $T_S$ divided by the proportion of radial glia that are in S-phase, given by the equation $T_c = T_S/(BrdU^+/BrdU^-)$.

**$Nfix^{fl/fl}$; $Nfib^{fl/fl}$; $Rosa26\text{-}CreER^{T2}$ tamoxifen treatment and cell analysis**

$Nfix^{fl/fl}$; $Nfib^{fl/fl}$ dams time-mated to $Nfix^{fl/fl}$; $Nfib^{fl/fl}$; *cre* sires were injected with 2 mg of tamoxifen dissolved in corn oil (10 mg/ml) at E10.5 and E11.5, and the embryos were collected at E15.5 and immersion-fixed in PFA. Quantification and imaging of total hippocampal $PAX6^+$ $TBR2^-$ nuclei and $TBR2^+$ nuclei was performed from two 100 µm sampling fields spanning the width of the hippocampus from two different levels along the rostrocaudal axis of the ammonic neuroepithelium. Fluorescent sections were imaged for this experiment using a 20X objective on a spinning disk confocal microscope. For analysis of $NFIX^-NFIB^+$ clones in the hippocampus of $Nfix^{fl/fl}$; $Nfib^{fl/fl}$; *cre* mice, sections were imaged using a 40X objective, on a spinning disk confocal microscope, through a depth of 10 µm (consecutive 1 µm z-steps). The z-stack was then flattened and the analysis was performed so that the proportion of $NFIB^+$ nuclei expressing TBR2 in the VZ/SVZ was compared to an adjacent region where VZ/SVZ nuclei were $NFIX^-$ $NFIB^-$. A minimum of two $NFIX^-NFIB^+$ clones were analyzed per animal.

**Quantitative real-time PCR (qPCR)**

The E13.5 medial cortex (hippocampal primordium and medial neocortex) or entire E16.5 hippocampal primordium of $Nfix^{-/-}$ and $Nfix^{+/+}$ littermates were microdissected and snap frozen. RNA was extracted (RNeasy Micro Kit, Qiagen, Valencia, CA) and reverse transcription was performed using Superscript III (Invitrogen) with 1 µg of total RNA using random hexamers according to manufactures protocol. qPCR was performed using SYBR green (Qiagen) and 500 nM of the *Insc* forward primer (5' CACTTTGCTCCTAGCTTCTGGA 3') and reverse primers (5'CCCAATCTGCAGCAATGCCT 3'). Expression of *Insc* in $Nfix^{-/-}$ and $Nfix^{+/+}$ littermates is expressed relative to the housekeeping gene *Glyceraldehyde-3-phosphate dehydrogenase* (*Gapdh*), which is presented as proportion of *Gapdh* transcript levels. Each sample at E13.5 (n = 5) and E16.5 (n = 3) was also performed in technical triplicate.

**Plasmid construction**

Two CRISPR constructs encoding a single gRNA against the bacterial *lacZ* gene or mouse *Nfix* gene were used in this study. For the *lacZ* construct a previously published gRNA sequence targeting *lacZ* (5'TGCGAATACGCCCACGCGATCGG;

underlined nucleotides, PAM motif) was used (Platt et al., 2014; Kalebic et al., 2016). To design a gRNA against the mouse *Nfix* gene, we used software from DNA 2.0 to generate a gRNA sequence that recognises within exon 2 of *Nfix* (5'TGAGTTCCACCCGTTTATCGAGG). DNA oligonucleotides encoding the *lacZ* and *Nfix* gRNA sequences (as above but excluding the PAM motif) were then ligated into the pD1321-AP plasmid (DNA2.0). In this plasmid the hU6 promoter controls expression of the gRNA, and a CAG promoter controls the expression of the CAS9-2A-PaprikaRFP cassette. For the rescue experiment a construct expressing full-length mouse INSC was generated by PCR amplifying the INSC open reading frame from IMAGE clone 4211657 into pCAGIG as described elsewhere (Petros et al., 2015). Other constructs used in this study were full-length NFIX pCAGIG, NFIB pCAGIG and NFIA pCAGIG constructs (Piper et al., 2010; Piper et al., 2011; Piper et al., 2014).

**Reporter gene assays**

The constructs used in the luciferase assays were NFIX pCAGIG, NFIB pCAGIG and NFIA pCAGIG expression constructs, an empty vector control pCAGIG and a luciferase construct (1358 base pairs) spanning –1078 base pairs to +279 base pairs from the transcriptional start site (TSS) of the mouse *Insc* promoter (UCSC genome browser track *uc009jii.2*, GRCM38/mm10). DNA was transfected into Neuro2A cells ($1*10^4$ cells) in a 96 well plate using Lipofectamine 2000 (Invitrogen), and Cypridina luciferase was added to each transfection as an internal control. After 24 h luciferase activity was measured using a dual luciferase system (Switchgear Genomics, Menlo Park, CA). Each condition, for each experiment, was performed in technical triplicate, and the experiment itself was replicated 5 times. Neuro2A cells were purchased from Sigma, and had been authenticated and tested for contamination.

**Analysis of ChIP-seq dataset**

The peaks from the ChIP-seq experiment using a pan-NFI antibody that was performed on embryonic stem cell-derived neural stem cells (Mateo et al., 2015; Supplementary Table 3, NFI tab) were annotated to the nearest gene using ChIPSeeker (Yu et al., 2015). Specifically, the following command was used: annotatePeak(chipPeaks, tssRegion = c(-3000, 1000), TxDb = txdb) where 'chipPeaks' is the bed file containing the locations of all peaks and 'txdb'

is TxDb.Mmusculus.UCSC.mm9.knownGene (Carlson and Maintainer, R package version 3.2.2). The 'distance to TSS' value in the resulting annotation file was used to refine the search to identify NFI proteins bound 5000 base pairs downstream (a minimum distance of -5000 base pairs) or 1000 base pairs upstream (a maximum distance of 1000 base pairs) of a TSS. The resulting genes associated with the NFI bound TSSs were then cross-referenced with the genes identified as misregulated in all three microarray datasets to identify key NFI target genes.

**ChIP-qPCR**

Whole E14.5 mouse forebrains were dissociated and fixed in 1% formaldehyde for 8 minutes. Nuclei were lysed and chromatin sonicated using 8 cycles (30s ON/30s OFF) of the Bioruptor Pico (Diagenode, Belgium) so that the majority of chromatin was between 100-500 base pairs in length. Immunoprecipitation was performed with 8 µg of goat anti-NFI (sc-30918, Santa Cruz) or 8 µg of goat IgG (AB-108-C, R&D Systems) control antibody coupled to 40 ul of Protein G Dynabeads (10003D, Thermo Fisher Scientific). DNA purification was performed using Qiagen PCR purification kit. ChiP-DNA was quantified using SYBR Green qPCR. A primer set for the *Insc* promoter was used (Forward: 5'TTAGCATCAAGAGCTCAGGACATT, Reverse: 5' TGCCAAGAAAAGACAGTTCACCA) as well as a negative control primer set in a gene desert region devoid of histone modification marks and transcription factor binding (Active Motif, #71011). Enrichment of NFI in the INSC promoter was calculated relative to IgG control using the delta CT method, and was further normalised to the negative control primer set to negate non-specific enrichment caused by residual, undersonicated chromatin. All primers for ChIP-PCR were used at a final concentration of 300 nM.

**Statistical analyses**

Sample size was determined to provide 80% power, and a type I error rate of 5% for the expected effect size, which varied per experiment. Two-tailed unpaired Students *t* tests were performed when comparing two groups. For experiments with comparisons between more than two groups ANOVAs were first performed, followed by multiple comparisons analysis, where a pooled estimate of variance was used if appropriate, and statistical significance was corrected for using the Holm-Sidak method in Prism 6.0 (Graphpad). All data that was analysed using Students *t* tests was performed with

a minimum sample size of 4 and assumed to be normally distributed. For analysis of the *Insc* qPCR data at E16.5, and ChIP-qPCR data, a sample size of 3 was analysed. In this case we did not assume a normal distribution of the data and, as such, we performed a one-sided Mann-Whitney U test in Prism 6.0. Because the test was based on a directional hypothesis (validating existing microarray or sequencing data), the one-sided test was justified. When the sample size is 3, the minimum *p*-value achievable from this nonparametric test is 0.05. All data analysis was performed blind to the genotype.

## Supplementary material references

**Cameron, H. A. and McKay, R. D.** (2001) 'Adult neurogenesis produces a large pool of new granule cells in the dentate gyrus', *J Comp Neurol* **435**(4): 406-17.

**Heng, Y. H., McLeay, R. C., Harvey, T. J., Smith, A. G., Barry, G., Cato, K., Plachez, C., Little, E., Mason, S., Dixon, C. et al.** (2014) 'NFIX regulates neural progenitor cell differentiation during hippocampal morphogenesis', *Cereb Cortex* **24**(1): 261-79.

**Kalebic, N., Taverna, E., Tavano, S., Wong, F. K., Suchold, D., Winkler, S., Huttner, W. B. and Sarov, M.** (2016) 'CRISPR/Cas9-induced disruption of gene expression in mouse embryonic brain and single neural stem cells in vivo', *EMBO Rep* **17**(3): 338-48.

**Kempermann, G., Kuhn, H. G. and Gage, F. H.** (1997) 'More hippocampal neurons in adult mice living in an enriched environment', *Nature* **386**(6624): 493-5.

**Martynoga, B., Morrison, H., Price, D. J. and Mason, J. O.** (2005) 'Foxg1 is required for specification of ventral telencephalon and region-specific regulation of dorsal telencephalic precursor proliferation and apoptosis', *Dev Biol* **283**(1): 113-27.

**Petros, T. J., Bultje, R. S., Ross, M. E., Fishell, G. and Anderson, S. A.** (2015) 'Apical versus Basal Neurogenesis Directs Cortical Interneuron Subclass Fate', *Cell Rep* **13**(6): 1090-5.

**Piper, M., Barry, G., Harvey, T. J., McLeay, R., Smith, A. G., Harris, L., Mason, S., Stringer, B. W., Day, B. W., Wray, N. R. et al.** (2014) 'NFIB-mediated repression of the epigenetic factor Ezh2 regulates cortical development', *J Neurosci* **34**(8): 2921-30.

**Piper, M., Barry, G., Hawkins, J., Mason, S., Lindwall, C., Little, E., Sarkar, A., Smith, A. G., Moldrich, R. X., Boyle, G. M. et al.** (2010) 'NFIA controls telencephalic progenitor cell differentiation through repression of the Notch effector Hes1', *J Neurosci* **30**(27): 9127-39.

**Piper, M., Harris, L., Barry, G., Heng, Y. H., Plachez, C., Gronostajski, R. M. and Richards, L. J.** (2011) 'Nuclear factor one X regulates the development of multiple cellular populations in the postnatal cerebellum', *J Comp Neurol* **519**(17): 3532-48.

**Platt, R. J., Chen, S., Zhou, Y., Yim, M. J., Swiech, L., Kempton, H. R., Dahlman, J. E., Parnas, O., Eisenhaure, T. M., Jovanovic, M. et al.** (2014) 'CRISPR-Cas9 knockin mice for genome editing and cancer modeling', *Cell* **159**(2): 440-55.

**Seib, D. R., Corsini, N. S., Ellwanger, K., Plaas, C., Mateos, A., Pitzer, C., Niehrs, C., Celikel, T. and Martin-Villalba, A.** (2013) 'Loss of Dickkopf-1 restores neurogenesis in old age and counteracts cognitive decline', *Cell Stem Cell* **12**(2): 204-14.

**Wojtowicz, J. M. and Kee, N.** (2006) 'BrdU assay for neurogenesis in rodents', *Nat Protoc* **1**(3): 1399-405.

**Yu, G., Wang, L. G. and He, Q. Y.** (2015) 'ChIPseeker: an R/Bioconductor package for ChIP peak annotation, comparison and visualization', *Bioinformatics* **31**(14): 2382-3.

**Zigman, M., Cayouette, M., Charalambous, C., Schleiffer, A., Hoeller, O., Dunican, D., McCudden, C. R., Firnberg, N., Barres, B. A., Siderovski, D. P. et al.** (2005) 'Mammalian inscuteable regulates spindle orientation and cell fate in the developing retina', *Neuron* **48**(4): 539-45.